Propagation of flexural waves at the interface between floating plates

Hyuck Chung and Colin Fox
Department of Mathematics, University of Auckland
Auckland, New Zealand

ABSTRACT

We present a theoretical study of wave propagation in two adjoining floating plates of different flexural rigidity, such as fast-ice sheets that abut across a pressure ridge, etc. Analytical formulas for the transmission and reflection coefficients for various conditions at the interface are obtained using the Wiener-Hopf technique for the case of semi-infinite elastic plates joined by a straight line. Solutions are scaled using the well-known characteristic length and time for an infinite floating plate, then categorized according to non-dimensional wave frequency that is independent of physical parameters. Thus the results give a relationship between scale-model experiments and real-sized structures.

KEY WORDS: Elastic plate; flexural waves; ice sheets; scaling; Wiener-Hopf.

INTRODUCTION

The shore-fast sea ice around Antarctica seasonally forms vast sheets that appear relatively featureless, and homogeneous, to the casual observer. However, closer inspection reveals that the ice sheets have substantial inhomogeneity at many length scales.

The ice sheet is typically a composite of floes that have frozen together after initial freezing and apparent break-up during winter. Each floe is typically tens of metres or kilometres across and often has very uniform thickness giving an abrupt change of thickness between some adjacent floes. The abutting of floes can occur across regions of frozen sea-water or ice rubble, or with pressure ridges when the floes are forced together, or partially refreezing cracks when the floes are moving apart. Stresses within the ice sheet, due to wind or current forcing, or due to thermal effects, cause further inhomogeneity in the form of pressure ridges, cracking, or finger jointing. These structures are most visible around islands or headlands where stress concentration occurs. However, cracking in the ice sheet, perhaps only partially through the thickness of the sheet, is prevalent and can occur with tens-of-metres spacing by the summer when wave-induced break-up typically occurs. Brine drainage pores give further structure to the ice sheet over metre scales.

The flexural gravity waves that propagate in the ice sheet, corresponding to ocean waves, have wavelengths of tens to hundreds of metres for typical thicknesses of first-year sea ice. Consequently the wave propagation, in the ice sheet at least, occurs in a medium with significant structure over the scale of wavelengths. Our interest is in modelling flexural wave propagation in an inhomogeneous ice sheet with particular interest in the scattering of wave energy, and the effective mechanical properties of a homogeneous sheet that would allow calculation of the unscattered wave component. In this paper we take a first step towards a comprehensive model by solving for the change in wave field across a single straight-line interface between large floes, allowing for changes in thickness with an open (cracked) or joined (refrozen) interface.

Mathematical modeling of ice sheets of large scale in marginal ice zone is mainly concerned with propagation of wave energy from the ocean which affects the breaking-up process of the ice sheets. For many years the formation and break-up of sea ice have interested not only geophysicists but also mathematicians (Balmforth and Craster, 1999; Evans and Davies, 1968; Fox and Squire, 1994; Gol'dshtein and Marchenko, 1989; Marchenko, 1997; Squire, Robinson, Langhorne and Haskell, 1988), because despite a great deal of idealization of the physical conditions, there have been few analytical solutions to the boundary value problems. We here present examples of analytical solutions of one category of boundary value problems related to the dynamics of sea ice sheets and from that solution we consider scaling effects on the interaction between two ice sheets.

In this paper we study the wave propagation on the surface of ocean which is covered with two semi-infinite ice sheets or very large floating structures (VLFS) which give elastic responses for deflection of small amplitude and long wave length. The two plates are assumed to have different flexural rigidity and joined

at an infinite straight line which we call transition or interface. Our main focus is on the reflection and transmission coefficients of plane waves when a plane wave of a given frequency is obliquely incident from infinity.

We use the Wiener-Hopf technique (Noble, 1958) to derive analytical solutions of the problem. Evans and Davies (1968) used the Wiener-Hopf technique (Noble, 1958) to derive analytical formulas of the reflection and transmission coefficients of waves propagating from free ocean surface to a semi-infinite ice sheet. However, the formulas were explained to be too complicated for the numerical computation at the time. The first computation of formal solutions was shown by Fox and Squire (1990) using a computational mode matching technique. In Balmforth and Craster (1999) numerical computation of analytical solutions is carried out using quadrature computation of integral transforms. Chung and Fox (2002) showed that the solutions obtained by Evans and Davies (1968) could in fact be computed without numerical computation of integral transforms by finding roots of the dispersion equations. The formulas given in this paper can be directly implemented to computer codes without any numerical computational considerations such as numerical integrations.

The method of solution used in this article is different from that by Meylan (2001) and Wang, Ertekin and Riggs (1997) who used a Green's function of free surface to compute flexural motion of a VLFS. They were able to compute the flexural response of a plate or plates from numerical evaluation of integral representation of the solutions. Simple integral representation of the velocity potential of fluid have been used by Crighton (1979), Gol'dshtein and Marchenko (1989) and Marchenko (1997). In recent years, Grant and Lawrie (2000) and Norris and Wickham (1995) gave studies of acoustic wave propagation in a fluid-loaded elastic plate with varying rigidity using the Wiener-Hopf technique. Lawrie and Abrahams (1999) used an orthogonality relation of the mode-expansion of solutions to derive numerical solution, which is closely related to the method by Fox and Squire (1994).

In this article, it is assumed that the deflection of ocean surface is small so that water can be modelled as incompressible and irrotational and the classic thin plate theory can be applied to the ice sheets, that is, ice sheet is modelled as a thin elastic plate (Kerr and Palmer, 1972). We deal with a time harmonic system by assuming existence of an incident wave from the infinity that is harmonic in time. At the joint of two ice sheets, the edges may be either free to move or frozen continuously. We by following and extending the method by Evans and Davies (1968) show that we can deal with changes of edge conditions without going back to the original differential equations. Furthermore, we apply the scaling scheme shown by Fox (2000) to categorize the solutions by non-dimensional wave frequency, which is insensitive to physical parameters, such as thickness of the plate. Hence, the non-dimensional values obtained here may help to design and evaluate scale-model experiments on ice sheets or floating structures.

MATHEMATICAL FORMULATION

We consider dynamics of two semi-infinite homogeneous thin plates joined at $x = 0$ as shown in Fig. 1. The flexural rigidity of the ice sheets in $x < 0$ and $x > 0$ are denoted by D_1 and D_2 respectively. The flexural rigidity is calculated using $D_i = Eh_i^3/12\left(1-\nu^2\right)$, where h_i, $i = 1, 2$ are the thickness of the plates in $x < 0$ and $x > 0$ respectively. ν is Poisson's ratio and E is effective Young's modulus that is constant in the plate. A

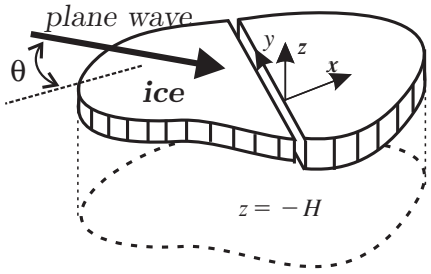

Fig.1 Schematics of the interaction of two semi-infinite plates with a straight line interface.

plane wave of radial frequency ω is coming from $x = -\infty$ at an angle θ. We assume that amplitude and frequency of the incident wave are small and low enough so that the water can be assumed to be incompressible and irrotational, and the ice sheets can be modelled as an elastic thin plate. Then, vertical displacement of the plates, $w(x, y, t)$, and velocity potential of water, $\phi(x, y, z, t)$ satisfy following partial differential equations.(Evans and Davies, 1968; Fox and Squire, 1994),

$$\left.\begin{array}{c} p = D_1\nabla^4_{x,y}w + \bar{m}_1\left(w_{tt}+g\right), \text{ for } x<0, \\ p = D_2\nabla^4_{x,y}w + \bar{m}_2\left(w_{tt}+g\right), \text{ for } x>0, \\ w_t = \phi_z, \\ \rho\phi_t + \rho g w + p = 0, \\ \phi_z = 0 \quad \text{at } z = -H, \end{array}\right\} \text{at } z = 0 \qquad (1)$$
$$\nabla^2_{x,y,z}\phi = 0 \text{ in the water.}$$

g, ρ and p are acceleration due to the gravity, mass density of sea water and pressure acted on the surface of the water respectively. The mass density of each plate is denoted by $m_i = \rho_{\mathrm{i}} h_i$ (ρ_{i} is the mass density of the ice), $i = 1, 2$ respectively. We assume that there exists an incoming plane wave obliquely incident from infinite that is harmonic in time, that is, at $x = -\infty$ we have $\mathrm{i}\, I \exp \mathrm{i}\left(\lambda x + \omega t\right)$, where I is amplitude of the wave (i is there to simplify the calculations later) and the wave number λ is determined by the incident angle of the plane wave to the x-axis. Since the system of the equations given in Eq. 1 are linear with respect to $\phi(x, y, z, t)$, we may express the solution as

$$\phi(x, y, z, t) = \mathrm{Re}\left[\phi(x, z, \omega)\, e^{\mathrm{i}(ky+\omega t)}\right]$$

where $\phi(x, z, \omega)$ (or $\phi(x, z)$ for simplicity) is the complex function of amplitude of the solution and k denotes the wave number in the y-axis, i.e., $k = \lambda' \sin\theta$, θ being the incident angle as depicted in Fig. 1.

We scale (or non-dimensionalize) the system of equations given above using characteristic length and characteristic time denoted by l_i and t_i, $i = 1, 2$ respectively. The subscript $i = 1$ corresponds to the plate for $x < 0$ and $i = 2$ for $x > 0$ and characteristic length and characteristic time are defined as

$$l_i = \left(\frac{D_i}{\rho g}\right)^{1/4}, \quad t_i = \sqrt{\frac{l_i}{g}}.$$

We also define the ratio of each characteristic value, $l_{\mathrm{r}} = l_1/l_2$ and $t_{\mathrm{r}} = t_1/t_2$, then the ratio of the flexural rigidity is

$$\frac{D_1}{D_2} = l_{\mathrm{r}}^4 = \left(\frac{h_1}{h_2}\right)^3.$$

We here assume that $l_{\mathrm{r}} < 1$, i.e., the plate on the right is more rigid than the other. l_{r} may be zero when $x < 0$ is free-surface.

It is assumed that $D_2 > 1$ so that l_r is always well defined. If we denote the non-dimensional variables with the bar, then the non-dimensionalized variables of space and time using l_2 are

$$(\bar{x}, \bar{y}, \bar{z}) = \frac{1}{l_2}(x, y, z), \ \bar{t} = \frac{t}{t_2}.$$

We omit the bar to avoid the clutter from now. Then, the system of equations given in Eq. 1 scaled by l_2 for $x < 0$ and $x > 0$ become

$$\begin{aligned} \left\{ l_\mathrm{r}^4 \left(\partial_x^2 - k^2\right)^2 - m_1\omega^2 + 1 \right\} \phi_z(x,0) &= \omega^2 \phi(x,0) \\ \left\{ \left(\partial_x^2 - k^2\right)^2 - m_2\omega^2 + 1 \right\} \phi_z(x,0) &= \omega^2 \phi(x,0) \end{aligned} \tag{2}$$

respectively. The mass density terms are now $m_i = \bar{m}_i/\rho l_2$, $i = 1, 2$. Note that $\phi(x, z)$ satisfy Helmholtz's equation for $-H < z < 0$,

$$\left(\frac{\partial^2}{\partial x^2} + \frac{\partial^2}{\partial z^2} - k^2 \right) \phi(x, z) = 0.$$

SOLUTION USING THE WIENER-HOPF TECHNIQUE

We derive scaled version of the reflection and transmission coefficients from the system of equations given by Eq. 2 using a slightly modified version of the standard Wiener-Hopf technique shown by Chung and Fox (2002). We apply the Fourier transform to the differential equations of ϕ in the respective domains $x < 0$ and $x > 0$, which are defined as

$$\begin{aligned} \Phi_+(\alpha, z) &= \int_0^\infty \phi(x, z)\, e^{\mathrm{i}\,\alpha x} dx, \\ \Phi_-(\alpha, z) &= \int_{-\infty}^0 \phi(x, z)\, e^{\mathrm{i}\,\alpha x} dx. \end{aligned} \tag{3}$$

We also denote the same transforms of $\phi_z(x, 0)$ in $x > 0$ and $x < 0$ by $\Phi'_\pm(x)$ respectively From the transforms of Laplace's equation and the condition at $z = -H$, we have

$$\left\{ \frac{\partial^2}{\partial z^2} - \left(\alpha^2 + k^2\right) \right\} \Phi_\pm(\alpha, z) = \pm \left\{ \mathrm{i}\,\alpha\phi(0, z) - \phi_x(0, z) \right\}.$$

Note that the functions $\Phi^\pm(\alpha, z)$ are regular in $\mathrm{Im}\,\alpha > 0$ and $\mathrm{Im}\,\alpha < 0$ respectively Hence, the solutions of the ordinary differential equations with the fixed bottom surface condition are written as

$$\Phi_\pm(\alpha, z) = \Phi_\pm(\alpha, 0) \frac{\cosh\gamma(z + H)}{\cosh\gamma H} \pm g(\alpha, z) \tag{4}$$

where $\gamma = \sqrt{\alpha^2 + k^2}$ and $g(\alpha, z)$ is a function determined by $\{\phi_x(0, z) - \mathrm{i}\,\alpha\phi(0, z)\}$,

$$\begin{aligned} g(\alpha, z) &= h(\alpha, z) - h(\alpha, 0) \frac{\cosh\gamma(z + H)}{\cosh\gamma H}, \\ h(\alpha, z) &= \int^z \frac{\sinh\gamma(z - \zeta)}{\gamma} \left\{ \phi_x(0, \zeta) - \mathrm{i}\,\alpha\phi(0, \zeta) \right\} d\zeta. \end{aligned}$$

Note that $\mathrm{Re}\,\gamma > 0$ when $\mathrm{Re}\,\alpha > 0$ and $\mathrm{Re}\,\gamma < 0$ when $\mathrm{Re}\,\alpha < 0$. We have, by differentiating the both sides of Eq. 4 with respect to z at $z = 0$

$$\Phi'_\pm(\alpha) = \Phi_\pm(\alpha)\gamma\tanh\gamma H \pm g_z(\alpha, 0) \tag{5}$$

where $\Phi'_\pm(\alpha)$ is the z-derivative of $\Phi_\pm(\alpha, z)$ at $z = 0$ which is denote by $\Phi_\pm(\alpha)$ respectively.

Applying the same integral transforms given by Eq. 3 to the plate equations in $x < 0$ and $x > 0$ we obtain

$$\left\{ l_\mathrm{r}^4\gamma^4 - m_1\omega^2 + 1 \right\} \Phi'_-(\alpha) - \omega^2\Phi_-(\alpha) = -P_1(\alpha), \tag{6}$$

$$\left\{ \gamma^4 - m_2\omega^2 + 1 \right\} \Phi'_+(\alpha) - \omega^2\Phi_+(\alpha) = P_2(\alpha), \tag{7}$$

where

$$P_j(\alpha) = D_j \left[c_3^j - ic_2^j\alpha - \left(\alpha + 2k^2\right)\left(c_1^j - ic_0^j\alpha\right) \right], \ j = 1, 2,$$
$$c_i^1 = \frac{\partial^i \phi_z(0-,0)}{\partial x^i}, \ c_i^2 = \frac{\partial^i \phi_z(0+,0)}{\partial x^i}, \ i = 0, 1, 2, 3.$$

From Eqs. 5~7 we have

$$f_1(\gamma)\Phi'_-(\alpha) + C_1(\alpha) = 0 \tag{8}$$

$$f_2(\gamma)\Phi'_+(\alpha) + C_2(\alpha) = 0 \tag{9}$$

where

$$\begin{aligned} f_1(\gamma) &= l_\mathrm{r}^4\gamma^4 - m_1\omega^2 + 1 - \frac{\omega^2}{\gamma\tanh\gamma H}, \\ f_2(\gamma) &= \gamma^4 - m_2\omega^2 + 1 - \frac{\omega^2}{\gamma\tanh\gamma H}, \\ C_1(\alpha) &= -\frac{\rho\omega^2 g_z(\alpha, 0)}{\gamma\tanh\gamma H} + P_1(\alpha), \\ C_2(\alpha) &= \frac{\rho\omega^2 g_z(\alpha, 0)}{\gamma\tanh\gamma H} - P_2(\alpha). \end{aligned}$$

Functions f_1 and f_2 are called *dispersion* functions and zeros of these functions are the primary tools of our method of deriving the solutions. How to compute the zeros of the dispersion functions are given by Chung and Fox (2002) and Fox and Chung (1998). The zeros of f_1 and f_2 are in pairs of positive and negative and complex conjugates. There are two real zeros due to tanh function and infinite number of pure imaginary zeros due to tan function. In addition to real and pure imaginary zeros, from Rouché theorem (Carrier, Krook and Pearson, 1966, page 60) there are four complex zeros.

Functions $\Phi_z^-(\alpha, 0)$, and $\Phi_z^+(\alpha, 0)$ are defined in $\mathrm{Im}\,\alpha < 0$ and $\mathrm{Im}\,\alpha > 0$ respectively, however they can be extended in the whole plane defined by Eqs. 8 and 9 using the analytic continuation. Eqs. 8 and 9 show that the singularities of Φ_z^- and Φ_z^+ are determined by the positions of the zeros of f_1 and f_2, since $g_z(\alpha, 0)$ is bounded and zeros of $\gamma\tanh\gamma H$ are not the singularities of $\Phi_z^\pm$. We denote sets of singularities corresponding zeros of f_1 and f_2 by S_1 and S_2 respectively

$$\begin{aligned} S_j = \Big\{ \alpha \in \mathbb{C} \mid f_j(\gamma(\alpha)) = 0, \ \alpha = \sqrt{\gamma^2 - k^2}, \\ \text{either } \mathrm{Im}\,\alpha > 0 \text{ or } \alpha > 0 \Big\}. \end{aligned}$$

We indicate the roots of the dispersion function corresponding to the elements of S_j by the prime, for example if $\lambda \in S_1$ then λ' on the γ-plane satisfies $f_1(\lambda') = 0$. We find that Eqns. 6 and 7 together with the regions in which $\Phi_\pm$ are regular tell us that $\Phi_-(\alpha)$ is singular at a real negative wave number denoted by $-\lambda$ ($\lambda \in S_1$) and S_1, and $\Phi_+(\alpha)$ is singular at $\alpha = -q$ where $q \in S_2$.

At the moment the two functions $\Phi'_-(\alpha)$ and $\Phi'_+(\alpha)$ do not share the domains of regularity in the upper and the lower half planes separated by the real axis. We are able to manipulate the region of the regularity by adding or subtracting one (or more) singular part of the functions. Here, we subtract a singular part corresponding to $-\lambda$ from $\Phi'_-(\alpha)$ and from $\Phi'_+(\alpha)$, that is, denoting the modified functions $\Psi'_\pm(\alpha)$, we have

$$f_1(\gamma)\Psi'_-(\alpha) + C_1(\alpha) = 0, \tag{10}$$

$$f_2(\gamma)\Psi'_+(\alpha) - \frac{If_2(\lambda)}{\alpha + \lambda} + C_2(\alpha) = 0. \tag{11}$$

Then, considering infinitesimal dissipation and the time factor $\exp(+\mathrm{i}\,\omega t)$, the functions $\Psi'_-(\alpha)$ and $\Psi'_+(\alpha)$ are regular on the real axis, or more precisely, the real axis indented over the negative real wave numbers $-\lambda$, $-\mu$ and indented under the positive real wavenumbers λ, μ. Let $\mathcal{D}_+$ and $\mathcal{D}_-$ denote the upper and lower half of the α-plane that are sharing the indented region on the real axis described above and shown in Fig. 2. Then, we may now add the both sides of Eqs. 10 and 11 to derive a typical Wiener-Hopf equation which is defined on $\mathcal{D}_+ \cap \mathcal{D}_-$,

$$f_1(\gamma)\,\Psi'_-(\alpha) + f_2(\gamma)\,\Psi'_+(\alpha) - \frac{I f_2(\lambda)}{\alpha+\lambda} + C(\alpha) = 0 \qquad (12)$$

where $C = C_1 + C_2$.

We now follow the standard method of solution of the Wiener-Hopf equation, which requires the factorization of the two dispersion functions. We have from Weierstrass' factor theorem and the symmetry of the positions of the roots in S_1 and S_2,

$$\frac{f_2}{f_1} = K(\alpha)\,K(-\alpha),$$
$$K(\alpha) = \left(\prod_{q=S_1} \frac{q'}{q+\alpha}\right)\left(\prod_{q=S_2} \frac{q+\alpha}{q'}\right). \qquad (13)$$

Note that $K(\alpha)$ is regular in the upper half plane and on the real axis except at $-\lambda$ and $-\mu$. Then, Eq. 12 becomes

$$f_2\left[f\Psi'_+ - \frac{f_2(\lambda)\,I}{\alpha+\lambda} + C\right] = -f_1\left[f\Psi'_- + \frac{f_2(\lambda)\,I}{\alpha+\lambda} - C\right] \qquad (14)$$

where $f(\gamma) = f_2(\gamma) - f_1(\gamma)$. Note that the splitting is actually performed on $f_1\gamma\sinh\gamma H$ and $f_2\gamma\sinh\gamma H$ which are none zero at $\gamma = 0$.

Then Eq. 14 can be rewritten as

$$\begin{aligned} &K(\alpha)\,[f\Psi'_+ + C] - \left(K(\alpha) - \tfrac{1}{K(\lambda)}\right)\tfrac{f_2(\lambda')I}{\alpha+\lambda} \\ &= -\tfrac{1}{K(-\alpha)}\,[f\Psi'_- - C] - \left(\tfrac{1}{K(-\alpha)} - \tfrac{1}{K(\lambda)}\right)\tfrac{f_2(\lambda')I}{\alpha+\lambda}. \end{aligned} \qquad (15)$$

We note that the infinite products in Eq. 13 converge in the order of q^{-5} as $|q|$ becomes large, thus numerical computation of $K(\alpha)$ does not pose any difficulties.

The left hand side of Eq. 15 is regular in $\mathcal{D}_+$ and the right hand side is regular in $\mathcal{D}_-$. Notice that a function is added to the both sides of the equation to make the right hand side of the equation regular in $\mathcal{D}_-$. The left hand side of Eq. 15 is $o(\alpha^4)$ as $|\alpha| \to \infty$ in $\mathcal{D}_+$, since $\Psi_z^+ \to 0$ and $K(\alpha) = O(1)$ as $|\alpha| \to \infty$ in $\mathcal{D}_+$. And the right hand side of Eq. 15 has the same analytic properties in $\mathcal{D}_-$. The Liouville's theorem (Carrier, Krook and Pearson, 1966, section 2.4) tells us that there exists a function, denoted by $J(\alpha)$, uniquely defined by Eq. 15, and function $J(\alpha)$ is a polynomial of degree three in the whole plane

$$J(\alpha) = d_0 + d_1\alpha + d_2\alpha^2 + d_3\alpha^3.$$

Equating Eq. 15 for $\Psi' = \Psi'_- + \Psi'_+$ gives

$$\Psi'(\alpha) = \frac{-F(\alpha)}{K(\alpha)\,f_1(\gamma)} \text{ or } -\frac{K(-\alpha)\,F(\alpha)}{f_2(\gamma)} \qquad (16)$$

where

$$F(\alpha) = J(\alpha) - \frac{I f_2(\gamma)}{(\alpha+\lambda)\,K(\lambda)}.$$

Notice that procedure from Eq. 14 to Eq. 15 eliminates the need of calculating C. We are now able to calculate using the following inverse Fourier transform

$$\phi_z(x,0) = \frac{1}{2\pi}\int_{-\infty}^{\infty} \Phi'(\alpha)\,e^{-\mathrm{i}\,\alpha x}\,d\alpha$$

where the integration path on the real axis is indented around the real singularities and may be closed in either the upper or lower half plane depending whether $x < 0$ or $x > 0$.

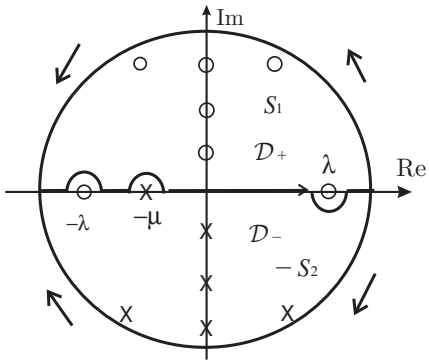

Fig.2 Schematics of the contour integration paths of the ivnerse Fourier transform and the positions (not to scale) of the corresponding roots in the α-plane. μ is not shown since it is not a singularity of the integrand.

For $x < 0$ we close the integral contour in $\mathcal{D}_+$ as depicted in Fig. 2, and put the incident wave back, then we have

$$\phi_z(x,0) = \mathrm{i}\,I e^{\mathrm{i}\,\lambda x} - \sum_{q\in S_1} \frac{\mathrm{i}\,F(q)\,q' R_1(q')}{qK(q)} e^{-\mathrm{i}\,qx}, \qquad (17)$$

where $R_1(q')$ is a residue of $[f_1(\gamma)]^{-1}$ at $\gamma = q'$

$$\begin{aligned} R_1(q') &= \left(\left.\frac{df_1(\gamma)}{d\gamma}\right|_{\gamma=q'}\right)^{-1} \\ &= \frac{\omega^2 q'}{(5l_{\mathrm{r}}^4 q'^4 + b_1)\,\omega^2 + H\left(\left(l_{\mathrm{r}}^4 q'^5 + b_1 q\right)^2 - \omega^4\right)}. \end{aligned} \qquad (18)$$

We used $b_1 = -m_1\omega^2 + 1$ and $f_1(q') = 0$ to simplify the formula. Displacement $w(x)$ can be obtained by multiplying $-\mathrm{i}/\omega$ to Eq. 17. The velocity potential $\phi(x,z)$ can be obtained using Eqs. 4 and 5,

$$\begin{aligned} \phi(x,z) = &\frac{\mathrm{i}\,I\cosh\lambda'(z+H)}{\lambda'\sinh\lambda' H} e^{\mathrm{i}\,\lambda x} \\ &- \sum_{q\in S_1} \frac{\mathrm{i}\,F(q)\,R_1(q')\cosh q'(z+H)}{qK(q)\sinh q' H} e^{-\mathrm{i}\,qx} \end{aligned}$$

where $\lambda' = \sqrt{\lambda^2 + k^2}$. And for $x > 0$, we derive $\phi_z(x,0)$ then $\phi(x,z)$ by closing the integral contour in $\mathcal{D}_-$ as depicted in Fig. 2,

$$\phi_z(x,0) = -\sum_{q\in S_2} \frac{\mathrm{i}\,K(q)\,F(-q)\,q' R_2(q')}{q} e^{\mathrm{i}\,qx}, \qquad (19)$$

$$\phi(x,z) = -\sum_{q\in S_2} \frac{\mathrm{i}\,K(q)\,F(-q)\,R_2(q')\cosh q'(z+H)}{q\sinh q' H} e^{\mathrm{i}\,qx},$$

where R_2 is a residue of $[f_2(\gamma)]^{-1}$ and its formula can be obtained by replacing the subscript 1 with 2 and l_{r} with 1 in Eq. 18. Notice

that from $R_j \sim O\left(q^{-9}\right)$ coefficients of ϕ_z decay as $O\left(q^{-6}\right)$ as $|q|$ becomes large, thus the displacement is bounded up to the fourth x-derivatives. The coefficients of ϕ, have extra $1/q' \tanh q'H$ term which is $O\left(q^4\right)$, hence the coefficients decay as $O\left(q^{-2}\right)$ as $|q|$ becomes large. Therefore, ϕ is bounded everywhere including at $x = 0$.

TRANSITION CONDITIONS

The four coefficients of $J(\alpha)$ are determined by physical conditions at $x = 0$, which we call transition conditions. We consider two kinds of conditions at the interface, open crack and continuously joined transition.

Let boundary differential operators acting on the displacement at the interface, $x = 0+$ and $x = 0-$, that corresponds to the effective shear force intensity and the bending moment by B_1 and B_2 respectively, Then, the transition conditions are expressed by displacement $w|_{x=0\pm}$, slope of the plate $w_x|_{x=0\pm}$, scaled effective shear force (Shames and Dym, 1991, section 6.3)

$$B_1 w|_{x=0+} = w_{xxx} - k^2(2-\nu) w_x \tag{20}$$

$$B_1 w|_{x=0-} = l_{\mathrm{r}}^4 \left\{ w_{xxx} - k^2(2-\nu) w_x \right\} \tag{21}$$

and scaled bending moment

$$B_2 w|_{x=0+} = w_{xx} - k^2 \nu w \tag{22}$$

$$B_2 w|_{x=0-} = l_{\mathrm{r}}^4 \left(w_{xx} - k^2 \nu w \right) \tag{23}$$

Since all possible transitions conditions are linear equations with respect to w, the transition conditions can be expressed by algebraic equations of column vector $\mathbf{d} = (d_0, d_1, d_2, d_3)$ made of the coefficients of polynomial J.

$$w|_{x=0\pm} = \mathcal{A}^{\pm} \cdot \mathbf{d} + \mathcal{B}^{\pm}, \;\; w_x|_{x=0\pm} = \mathcal{C}^{\pm} \cdot \mathbf{d} + \mathcal{D}^{\pm},$$
$$B_1 w_x|_{x=0\pm} = \mathcal{E}^{\pm} \cdot \mathbf{d} + \mathcal{F}^{\pm}, \;\; B_2 w_x|_{x=0\pm} = \mathcal{G}^{\pm} \cdot \mathbf{d} + \mathcal{H}^{\pm}$$

where $\mathcal{A}^{\pm}$, $\mathcal{C}^{\pm}$, $\mathcal{E}^{\pm}$ and $\mathcal{G}^{\pm}$ are row vectors, and $\mathcal{B}^{\pm}$, $\mathcal{D}^{\pm}$, $\mathcal{F}^{\pm}$ and $\mathcal{H}^{\pm}$ are scalar values that are calculated from Eqs. 17, 19, 20 and 22, and $\cdot$ is the vector inner product.

Open crack condition are $B_1 w_x|_{x=0\pm} = 0$ and $B_2 w_x|_{x=0\pm} = 0$. Then the coefficients of J are computed from

$$\begin{bmatrix} \mathcal{E}^- \\ \mathcal{E}^+ \\ \mathcal{G}^- \\ \mathcal{G}^+ \end{bmatrix} \mathbf{d} = - \begin{pmatrix} \mathcal{F}^- \\ \mathcal{F}^+ \\ \mathcal{H}^- \\ \mathcal{H}^+ \end{pmatrix}. \tag{24}$$

When the two plates have the same thickness, i.e., $l_{\mathrm{r}} = 1$, and transition is free to move, then we have one dispersion function $f_1(\gamma) = f_2(\gamma)$. Note that there is no need for factorization since, $K \equiv 1$. The sets of wave numbers S_1 and S_2 are the same. The incident wave does not automatically appear in this case since the wave number for incident wave and traveling wave are the same. Hence, Eq. 19 must be changed to

$$\phi_z(x,0) = \mathrm{i}\, I e^{\mathrm{i}\,\lambda x} - \sum_{q \in S_1} \frac{\mathrm{i}\, J(-q)\, q' R_2(q')}{q} e^{\mathrm{i}\, q x}.$$

Squire and Dixon (2000) used a Green's function satisfying the plate equation at $z = 0$ to derive analytical solutions for a case of normal incident wave.

Two *continuously joined* plates are expressed by following continuity conditions

$$B_1 w_x|_{x=0-} = B_1 w_x|_{x=0+}, \;\; B_2 w_x|_{x=0-} = B_2 w_x|_{x=0+},$$
$$w|_{x=0-} = w|_{x=0+}, \;\; w_x|_{x=0-} = w_x|_{x=0+}.$$

Then, $\mathbf{d}$ can be obtained from

$$\begin{bmatrix} \mathcal{A}^- - \mathcal{A}^+ \\ \mathcal{C}^- - \mathcal{C}^+ \\ \mathcal{E}^- - \mathcal{E}^+ \\ \mathcal{G}^- - \mathcal{G}^+ \end{bmatrix} \mathbf{d} = - \begin{pmatrix} \mathcal{B}^- - \mathcal{B}^+ \\ \mathcal{D}^- - \mathcal{D}^+ \\ \mathcal{F}^- - \mathcal{F}^+ \\ \mathcal{H}^- - \mathcal{H}^+ \end{pmatrix}. \tag{25}$$

We showed that the conditions at $x = 0\pm$ can be expressed by a matrix made of row vectors $\mathcal{A}^{\pm}$, $\mathcal{C}^{\pm}$, $\mathcal{E}^{\pm}$, $\mathcal{G}^{\pm}$ and a vector made of $\mathcal{B}^{\pm}$, $\mathcal{D}^{\pm}$, $\mathcal{F}^{\pm}$, $\mathcal{H}^{\pm}$. Hence, we may say that problems described by Eq. 1 are now reduced to algebraic Eqs. 24 and 25 and sets of wavenumbers calculated from the dispersion functions, S_1 and S_2.

REFLECTION AND TRANSMISSION COEFFICIENTS

At $|x| \to \infty$ the only the travelling waves of the displacement are left. Hence, we have a relation between the transmission and reflection coefficients

$$s\mathcal{T}^2 + \mathcal{R}^2 = 1 \tag{26}$$

where $\mathcal{T}$ and $\mathcal{R}$ are ratio between amplitude of displacement of transmitted and reflected wave and amplitude of incident wave. Setting $I = 1$ gives formulas for the transmission and reflection coefficients,

$$\mathcal{T} = \left| \frac{\mu' F(-\mu) R_2(\mu') K(\mu)}{\mu} \right|,$$
$$\mathcal{R} = \left| \frac{\lambda' F(\lambda) R_1(\lambda')}{\lambda K(\lambda)} \right|.$$

The multiplying factor s is

$$s = \frac{\mathrm{Re}(\mu)\, \lambda'^2 \sinh 2\lambda' H}{\mathrm{Re}(\lambda)\, \mu'^2 \sinh 2\mu' H} \times \frac{2\mu' H \left(\mu'^4 + b_2\right) + \left(5\mu'^4 + b_2\right) \sinh 2\mu' H}{2\lambda' H \left(l_{\mathrm{r}}^4 \lambda'^4 + b_1\right) + \left(5 l_{\mathrm{r}}^4 \lambda'^4 + b_1\right) \sinh 2\lambda' H}$$

The power-flow relation (26) holds for all transition conditions which do not introduce any potential energy to the system. We note that when $l_{\mathrm{r}} = 0$ and $m_1 = 0$ the formula for multiplying factor s is reduced to the one shown by Fox and Squire (1994) for ocean wave-ice interaction problem. The numerical computations given here are obtained using up to 80 zeros of f_1 and f_2 depending on the water depth, since the smaller H is, the faster the functions $K(\alpha)$ and R_1, R_2 converge.

Fig. 3 shows the reflection coefficient for $l_{\mathrm{r}} = 1$ and $m_1 = m_2 = 0$. We will justify setting the mass density to be zero in the following section. We notice that for $l_{\mathrm{r}} = 1$, the reflection coefficient reaches zero at a finite frequency around $\omega = 1$, which is confirmed by Squire and Dixon (2000) using a Green's function for an infinite plate floating on the surface of deep water. The zero reflection occurs at around $\omega = 1$ for a range of incident angle up to $\pi/3$ as shown in Fig. 3. The amplitude of the displacement, $|w(0\pm)|$, at the transition is given in Fig. 4 when the amplitude of the incident wave is one. Fig. 4 shows that at $\omega \sim 1$, the amplitude of the displacement of the ice sheets at $x = 0\pm$ are equal. The amplitude of displacement at $x = 0-$ is larger than that at $x = 0+$ when $\omega < 0$ and $|w(0+)|$ is smaller than $|w(0-)|$ when $\omega > 1$.

Figs. 5 and 6 show the reflection coefficients when $l_{\mathrm{r}} = 1/2$ for two different physical situations at the transition, open crack and

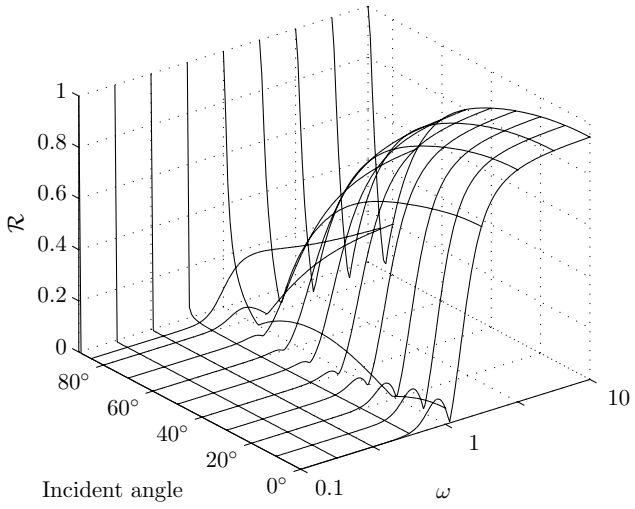

Fig. 3 The reflection coefficient as a function of the incident angle (in degrees) and the non-dimensional radial frequency ω (log-scale) when $l_{\rm r} = 1$ and $H = 2\pi$. The mass density term is set to be zero.

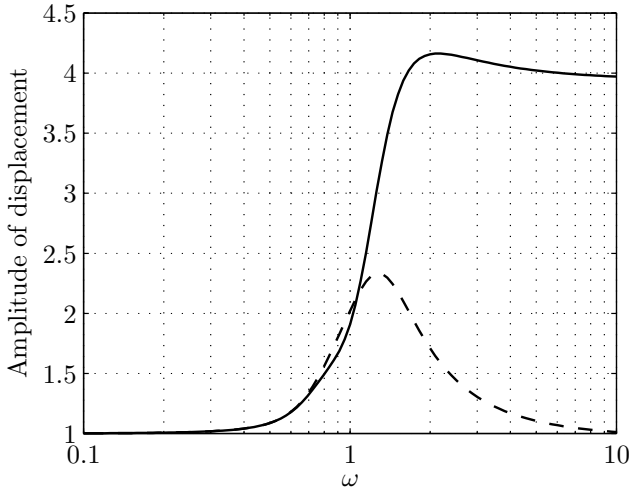

Fig. 4 Amplitude of the displacement at the transition $x = 0\pm$ when $l_{\rm r} = 1$. $|w\,(0-)|$ is solid line, and $|w\,(0+)|$ is dashed line.

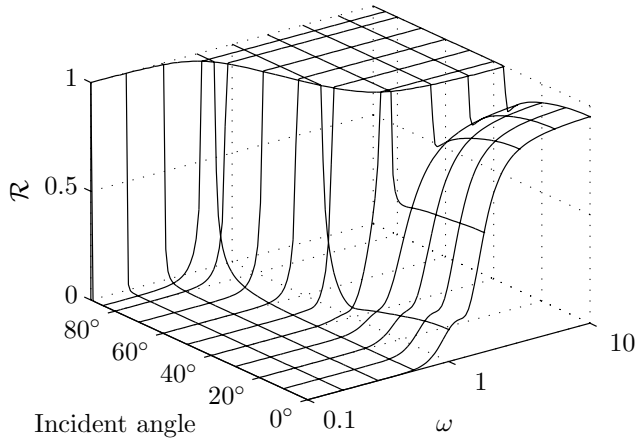

Fig. 5 Three dimensional graph of the reflection coefficient as a function of the non-dimensional radial frequency ω (log-scale) and the incident angle (in degree) when $l_{\rm r} = 1/2, H = 2\pi$ and the transition is free to move.

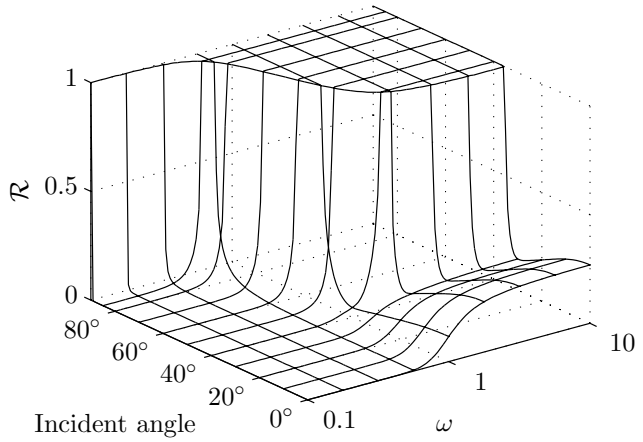

Fig. 6 Three dimensional graph of the reflection coefficient as a function of the non-dimensional radial frequency ω (log-scale) and the incident angle (in degrees) when $l_{\rm r} = 1/2, H = 2\pi$ and the transition is continuously joined.

continuous joint respectively. We find that there is little difference between the two graphs in the region $\{\omega < 1.3$ or $\theta > \pi/5\}$. Tha mass density terms are again set to be zero, $m_1 = m_2 = 0$.

EFFECTS OF NON-DIMENSIONALIZATION

We study the behaviour of the reflection coefficient under the scaling scheme.

From Figs. 3 and 4, we may categorize the reflection coefficient according to its behaviour and the non-dimensional frequency using the values. At $\omega < 0.7$ (low frequency), the open crack is virtually invisible to the incident waves. $0.7 < \omega < 1$, the plate on the right ($x > 0$) has larger displacement.

Figs. 7 and 8 show the curves of the reflection coefficient $\mathcal{R}$ versus the non-dimensional radial frequency ω for a various water depth and incident angles. We find that the reflection coefficient is not affected by the water depth that is greater than 2π for both open crack and continuous joint cases. Hence, we may say that non-dimensional water depth $H = 2\pi$ is *deep*. The graphs for $\theta = \pi/3$ in Figs. 7 and 8 show that at high incident angle, the transition conditions have no effects on the wave propagation.

Fig. 9 shows the reflection coefficients for various mass density terms for deep-water ($H > 2\pi$). We find that the mass density terms m_1 and m_2 have no qualitative effects on the reflection at the transition of the plates. Hence, for 'deep-water' we may consider only the cases when $m_1 = m_2 = 0$ for a typical range of non-dimensional mass density of an ice sheet around 0 to 0.1. For 'shallow-water' this omission of mass density terms may not be justified since the effects of changing H is as significant as those of the mass density. Then, the resulting dispersion functions f_1 and f_2 for deep-water, $H > 2\pi$, are completely independent of the physical parameters, mainly the thickness, of the ice sheets. The interaction of two ice sheets are now described only by the

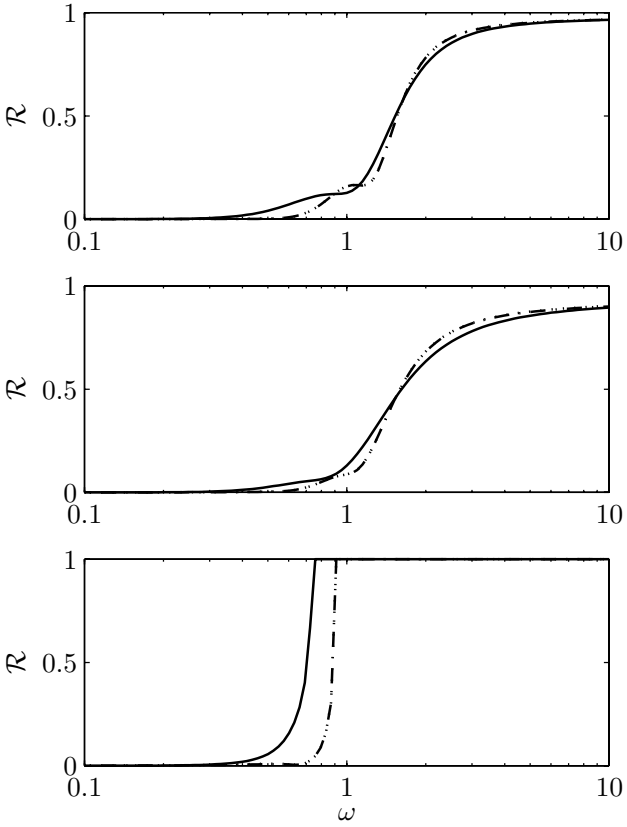

Fig. 7 The reflection coefficients for various non-dimensional water depth, $H = 0.2\pi$(solid curve), 2π(dash-dot curve), 4π(dotted curve). The transition conditions are *open crack* and the incident angles are from the top $0, \pi/6, \pi/3$. The curves for $H = 2\pi$ and 4π are indistinguishable. The parameters are $l_{\rm r} = (1/2)^{3/4}$ and $m_2 = 0.05, m_1 = m_2/2$.

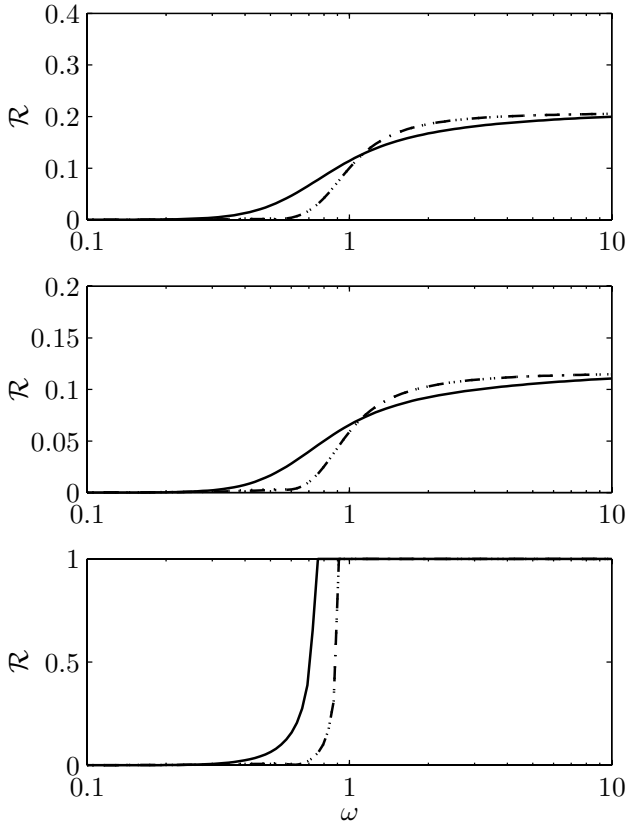

Fig. 8 The reflection coefficients for the same non-dimensional parameters as in Fig. 7, except the transition conditions are now *continuous joint*.

ratio of the two characteristic length $l_{\rm r}$.

Fig. 10 shows the changes in the reflection coefficient as the ratio of the characteristic length $l_{\rm r}$ varies. For open crack transition case the reflection reaches the same value as the frequency increases, where as the continuous transition case shows decrease in the reflection as $l_{\rm r}$ tends to one. Of course there will be no reflection of waves when $l_{\rm r} = 1$ for the continuous transition and the two curves of the reflection coefficient will become the same as $l_{\rm r}$ tends to zero for a finite value of l_2, i.e., the left hand side of the surface is free ocean surface.

Let ω_1 denote the non-dimensional radial frequency that are scaled by the characteristic time t_1, i.e., $\omega_1 = \omega t_{\rm r} = \sqrt{l_{\rm r}}$. Then, the unit radial frequency $\omega_1 = 1$ is $\omega = 1/\sqrt{l_{\rm r}}$. From the top graph of Fig. 10, we find using the value of $\omega_1 = 1$ that the curves of the reflection coefficients can be categorized into four regions of frequency according to their behaviour. First, low frequency, $\omega < 0.7$, at which virtually zero reflection for any values of $l_{\rm r}$. Second, $0.7 < \omega < 1/\sqrt{l_{\rm r}}$ (unit frequency normalized by t_1), at which the curves are 'wobbly'. Third, $1/\sqrt{l_{\rm r}} < \omega < 4$, at which the reflection increased steadily and rapidly. Fourth, high frequency, $4 < \omega$, at which the curves for all $l_{\rm r}$ reach the limit and

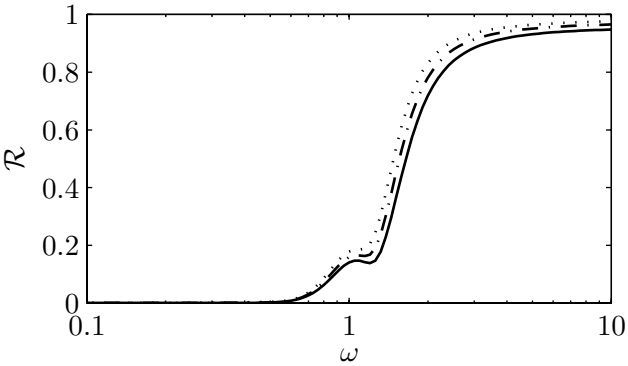

Fig. 9 Curves of the reflection coefficient versus non-dimensional radial frequency for various mass density factors. $m_1 = m_2/2$ and $m_2 = 0.1$ (dotted curve), 0.05 (dash-dot curve) and zero (solid curve). $\theta = 0$ and $H = 2\pi$.

stay unchanged. We notice from Fig. 10, there exist a frequency between 0.7 and $1/\sqrt{l_{\rm r}}$, at which the reflection coefficients for the two transition conditions are equal.

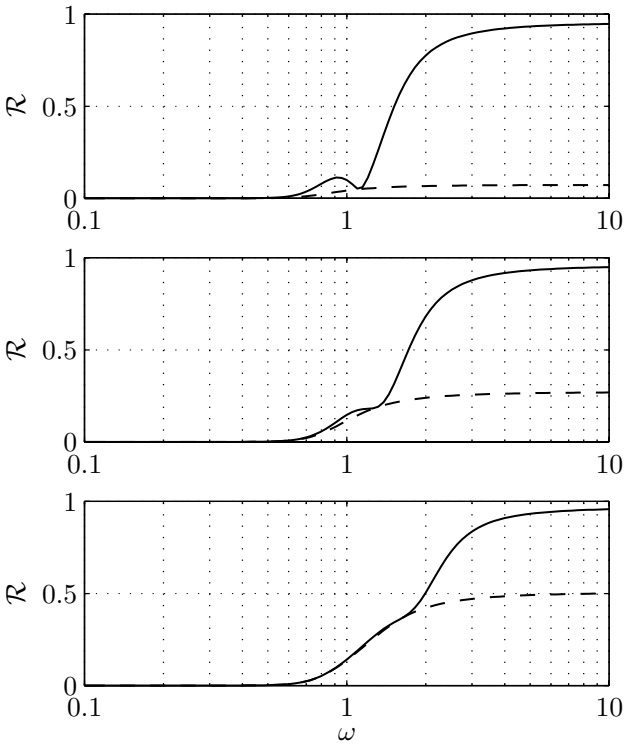

Fig. 10 The reflection coefficients versus non-dimensional radial frequency ω when $l_{\rm r} = 1/1.2, 1/2, 1/4$ (from the top) and open crack (solid) and continuous joint (dashed). Incident angle $\theta = 0$ and water depth $H = 2\pi$.

CONCLUSIONS

We have presented the analytical formulas and numerical computation of the coefficients of the mode expansion of the flexural waves in two semi-infinite plates. The coefficients are computed from the conditions at the transition of the two plates, which are expressed by a 4×4 matrix and 4 element vector. The formulas of the solutions can be directly turned into stable computer codes that can deal with various transition conditions by changing the matrix and vector of the transition conditions. We have shown that the Wiener-Hopf equation can be obtained directly from the Fourier transforms of the system of equations rather than assuming the modal expansion of the solution to find the analyticity of the Fourier transforms of the solution in $x < 0$ and $x > 0$. The splitting of f_2/f_1 is expressed by one function $K(\alpha)$ because of the symmetry of the positions of the singularities in $\mathcal{D}_-$ and $\mathcal{D}_+$, which simplifies the formulas of the solutions.

The space and time variables are non-dimensionalized using the characteristic length $l_i, i = 1, 2$, characteristic time $t_i, i = 1, 2$. The resulting solutions are insensitive to the change of ice thickness, hence we are able to set the mass density term to be zero and find that the water depth $H > 2\pi$ can be considered as deep. Using the graphs of the reflection coefficient $\mathcal{R}$ for various $l_{\rm r}$, we are able to categorize the wave propagation across a transition in two semi-infinite plate into four distinctive regimes by the values of the non-dimensional frequency $\omega = 0.7, 1/\sqrt{l_{\rm r}}, 4$. These values can be interpreted to ice sheets or floating structures of any thickness, such as scale-models created in a laboratory.

REFERENCES

Balmforth, NJ, and Craster, RV (1999). "Ocean waves and ice sheets," *J. Fluid Mech.*, Vol 395, pp 89–124.

Carrier, GF, Krook, M, and Pearson, CE (1966). *Functions of a Complex Variable, Theory and Technique,* McGrawHill, New York.

Chung, H, and Fox, C (2002). "Calculation of wave-ice interaction using the Wiener-Hopf technique," *New Zealand J. Math.*, In printing.

Crighton, DG (1979). "The free and forced waves on a fluid-loaded elastic plate," *J. Sound Vib.*, Vol 63, pp 225–235.

Evans, DV, and Davies, TV (1968). *Wave-Ice Interaction Repot1313.* Davidson Laboratory, Stevens Institute of Technology, Hoboken.

Fox, C, and Chung, H (1998). "Green's function for forcing of a thin floating plate," *Technical Report*, Vol 408, www.math.auckland.ac.nz/Research/DeptRep/reports.html, Department of Mathematics, University of Auckland.

Fox, C (2000). "Scaling laws for flexural waves in floating ice," *Proceedings of IUTAM Scaling Lows in Ice Mechanics and Ice Dynamics.* Fairbanks, Alaska, USA.

Fox, C, and Squire, VA (1990). "Reflection and transmission characteristics at the edge of shore fast sea ice," *J. Geophysical Research*, Vol 95, No C7, pp 11,629–11,639.

Fox, C, and Squire, VA (1994). "On the oblique reflexion and transmission of ocean waves at shore fast sea ice," *Phil. Trans. R. Soc. Lond*, Vol 347, No A, pp 185–218.

Gol'dshtein, RV, and Marchenko, AV (1989). "The diffraction of plane gravitational waves by the edge of an ice cover," *Prikl. Matem. Mekhan.*, Vol 53, No 6, pp 731–736.

Grant, AD, and Lawrie, JB (2000). "Propagation of fluid-loaded structural waves along a duct with smoothly varying bending characteristics," *Q. Jl Mech. appl. Math.*, Vol 53(2), pp 299–321.

Kerr, AD, and Palmer, WT (1989). "The deformations and stresses in floating ice plates," *Acta Mech.*, Vol 15, pp 15–72.

Lawrie, JB, and Abrahams, ID (1999). "An orthogonality relation for a class of problems with high-order boundary conditions; applications in sound-structure interaction," *Q. Jl Mech. appl. Math.*, Vol 52(2), pp 161–181.

Marchenko, AV (1997). "Flexural-gravity waev diffraction at linear irregularities in sheet ice," *Fluid mechanics.*, Vol 32, pp 548–560.

Meylan, MH (2001). "A variational equation for the wave forcing of floating thin plates," *Applied ocean research*, Vol 23, pp 195–206.

Noble, B (1958). *Methods Based on the Wiener-Hopf Technique for the Solution of Partial Differential Equations.* Pergamon Press, London.

Norris, AN, and Wickham, GR (1995). "Acoustic diffraction from the junction of two flat plates," *Proc. R. Soc. Lond. A*, Vol 451, pp 631–655.

Shames, IH, and Dym, CL (1991). *Energy and Finite Element Methods in Structural Mechanics.* Hemisphere Publishing Corporation, Bristol, PA, si units edition.

Squire, VA, and Dixon, TW (2000). "An analytic model for wave propagation across a crack in an ice sheet," *International Journal of Offshore and Polar Engineering*, Vol. 10, No. 3, 173–176.

Squire, VA, Robinson, W, Langhorne, PJ, and Haskell, TG (1988). "Vehicles and aircraft on floating ice," *Nature*, Vol 133, No 6169, pp 159–161.

Wang, S, Ertekin, RC, and Riggs, HR (1997). "Computationally efficient techniques in the hydroelasticity analysis of very large floating structures," *Computers and structures*, Vol. 62, No. 3, 603–610.